Efficient estimation of burst-mode LDA power spectra

Clara M. Velte[1], William K. George[2]

1: Department of Mechanical Engineering, Technical U. of Denmark, Kgs. Lyngby, Denmark, cve@mek.dtu.dk
2: CNRS, UML, U. Lille Nord de France, Villeneuve d'Asca France, georgewilliamk@gmail.com

Abstract The estimation of power spectra from LDA data provides signal processing challenges for fluid dynamicists for several reasons. Acquisition is dictated by randomly arriving particles which cause the signal to be highly intermittent. This both creates self-noise and causes the measured velocities to be biased due to the statistical dependence on the velocity and when the particle arrives. This leads to incorrect moments when the data are evaluated by arithmetically averaging. The signal can be interpreted correctly, however, by applying residence time weighting to all statistics, which eliminates the velocity bias effects. Residence time weighting should also be used to compute velocity spectra. The residence time-weighted direct Fourier transform can, however, be computationally heavy, especially for the large data sets needed to eliminate finite time window effects and given the increased requirements for good statistical convergence due to the random sampling of the data. In the present work, the theory for estimating burst-mode LDA spectra using residence time weighting is discussed and a practical estimator is derived and applied. A brief discussion on the self-noise in spectra and correlations is included, as well as one regarding the statistical convergence of the spectral estimator for random sampling. Further, the basic representation of the burst-mode LDA signal has been revisited due to observations in recent years of particles not following the flow (e.g., particle clustering), which was not covered in the previous theory. An efficient algorithm for computing the residence time weighted power spectra using Matlab is proposed and implemented. The algorithm is applied to two experiments, one with high data density (cylinder wake) and one with relatively low data density (axisymmetric turbulent jet). The burst-mode LDA spectra are compared to corresponding spectra from hot-wire data obtained in the same experiments, and to LDA spectra produced by the sample-and-hold methodology. The spectra computed from the residence-time weighted burst-mode algorithm proposed herein compare favorably to the hot-wire data for both experiments, independent of the LDA data density. The sample-and-hold spectrum produced from the same LDA data, however, is very different for the low data density due to frequency dependent filtering of the spectrum inherent in the method.

1. Introduction

The burst-mode LDA should be operated with at most one particle in the scattering volume, which means that for most of the time there are none [1]. Thus the burst-mode LDA can be assumed to sample whenever a particle passes through the scattering volume. This presents three challenges to interpreting the signal correctly:

Random (but velocity dependent) sampling: The particle arrivals dictate the sampling which is therefore non-uniform and velocity dependent. In other words, the sampling process and sampled process are not statistically independent.

Intermittent signal: The on-off nature of the signal changes dramatically the power spectrum if it is processed as an analog signal; and it produces incorrect moments if simply processed using arithmetic algorithms developed for data sampled at a fixed rate.

Velocity bias: The statistics can be significantly biased since the sampling process itself depends on the velocity. Since the probability of acquiring more samples per unit time increases with higher velocities, the bias is usually (but not always) towards higher velocities [2].

For the signal to be interpreted correctly and to avoid velocity bias, one must apply residence time-weighting to all statistical analysis [3]. Further, for time-series analysis, even though the randomly arriving particles eliminate aliasing (at least in principle), the self-noise from the random arrivals must be removed or it will dominate the spectra and correlations [4]. This paper will first review the theoretical basis for residence time weighting of all statistics. Then the theory will be used to develop a practical algorithm for the estimation of the power spectrum from burst-mode LDA data. A flaw in the earlier theory [1,3], the goal of which was to provide an unbiased and unaliased spectral estimator from the random samples, has been identified and corrected. The new methodology is illustrated using experiments in an axisymmetric turbulent far jet and a cylinder wake. The results are compared to corresponding hot-wire measurements and spectra from interpolated and re-sampled (sample-and-hold) LDA signals. Due to the random sampling, the variability of the spectral estimator is larger than for regularly sampled data, so this will also be discussed. Finally, a Matlab script is provided for computing burst-mode LDA spectra is provided in Appendix B.

2. Residence time weighting of the statistics

The problem of representing the burst-mode LDA signal has previously been addressed by considering the fluid particle motions, $\vec{x}(\vec{a},t)$, in Lagrangian space [3,5-7], and using a sampling function, $g(\vec{a})$, that samples the velocity at the initial spatial locations of the particle. Subsequent to this it was assumed that the flow was incompressible and that the sampling function could be transformed to Eulerian space. This part of the analysis appears to have been incorrect. Also the earlier analysis did not include the possible effects of the particles not following the flow. This is especially important since clustering of particles has been observed in recent years [8]; therefore this part of the analysis has also been reconsidered.

Considering the particle motions in Lagrangian space, the velocity as sampled by the LDA at location $\vec{x}$, say $\tilde{u}_{i0}(\vec{x},t)$, can be defined by

$$\tilde{u}_{i0}(\vec{x},t) = \iiint_{all\ space} u_i(\vec{a},t) g(\vec{a}) w\left(\vec{x} - \vec{X}[\vec{a},t]\right) d^3\vec{a} \tag{1}$$

where $u_i(\vec{a},t)$ is the velocity of the **particle** with initial position $\vec{a}$. $g(\vec{a})$ is a sampling function that describes whether a particle is present or not at position $\vec{a}$ at the arbitrarily chosen initial instant. The positions of the particles are given by their displacement field, say $\vec{X}[\vec{a},t]$. $w(\vec{x})$ is a weighting function that accounts for the finite extent of the measuring volume centered at location $\vec{x}$, and effectively 'turns on' when the particle enters the volume and 'turns off' when it leaves. The weighting function is dimensionless and must by definition yield the volume of the measuring volume when integrating across all space, i.e.,

$$V(\vec{x}) \equiv \iiint_{all\ space} w(\vec{x}') d\vec{x}'. \tag{2}$$

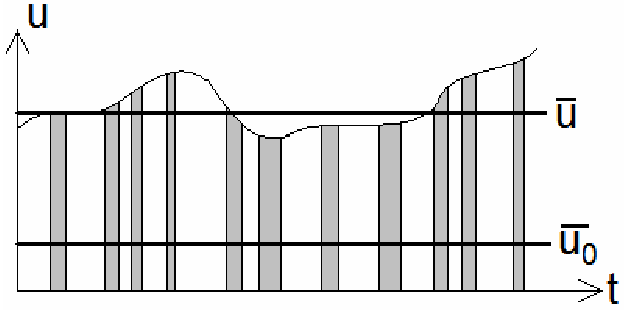

Figure 1: Sketch of velocity, u (curve), along with the interrupted sampled signal, u_0 (shaded areas), resulting from random arrivals of particles carried by the flow.

It has long been recognized that the intermittently sampled velocity (illustrated in Figure 1) yields biased and incorrect estimates of the moments such as the mean, ***unless it is treated as a time signal while it is 'on'*** [3,5-7]. The 'on-time' of the signal is given by

$$\iiint_{all\ space} g(\vec{a}) w\left(\vec{x} - \vec{X}[\vec{a},t]\right) d^3\vec{a} = \mu V \approx \frac{1}{T}\sum_{n=0}^{N-1} \Delta t_n \tag{3}$$

where $\mu = \overline{g(\vec{a})}$ is the expected number of particles per unit volume, T is the record length and V is the volume of the scattering volume. Hence, μV is the expected number of particles in the volume, but is also the percentage of the total time for which a particle is present.

As noted above, the remedy to the problem portrayed in Figure 1 is to account for the time that the signal is actually present. Thus the mean of the burst-mode signal is the mean of the volume-averaged velocity, but multiplied by μV (which is always less than unity); i.e.:

$$\overline{\tilde{u}_{i0}} = \overline{\iiint_{all\ space} u_i(\vec{a},t) g(\vec{a}) w\left(\vec{x} - \vec{X}[\vec{a},t]\right) d^3\vec{a}} = \mu V \,\overline{u_i} \approx \lim_{\substack{T\to\infty,\\ N\to\infty}} \frac{1}{T}\left\{\sum_{n=0}^{N-1} \int_{t_n}^{t_n+\Delta t_n} u_{i0}(t)\, dt\right\}, \tag{4}$$

where the time integral can be used to replace the ensemble average if the process is stationary. From this it is straightforward to see that the piecewise mean velocity integral can be best approximated by:

$$\bar{u}_i = \frac{\sum_{n=0}^{N-1} u_i(t_n)\Delta t_n}{\sum_{n=0}^{N-1} \Delta t_n} \tag{5}$$

where Δt_n is the residence (or transit) time for the n^{th} realization. Also it is clear at this point precisely which velocity, $\bar{u}_i$, is being measured: namely the *volume-averaged particle velocity*. Only if the particles are following the flow does this correspond to the volume-averaged Eulerian velocity.

Similar residence time weighted algorithms can be derived for all the single-time moments, and must be used when correlating burst-mode LDA data with continuous signals as well (like from hot-wires or pressure sensors), c.f. [1,9]. As noted by [6], the residence time can also be used to obtain the Fourier coefficients for spectral estimation; i.e., discretizing the finite time Fourier transform of the velocity signal yields:

$$\hat{u}_{iT}(f) = \int_0^T e^{-i2\pi f t} u_i(t) dt \approx \sum_{n=0}^{N-1} e^{-i2\pi f t_n} u_{i\,n}\, \Delta t_n \tag{6}$$

where the subscript T indicates that the quantity is evaluated over a finite time domain. The spectral estimator which can be derived from this is discussed in detail in section 4 below, following a discussion in the following section of the theoretical implications of the intermittency of the burst mode LDA output interpreted as a time signal.

3. Second order statistics

The two-time cross-correlation of the instantaneous burst-mode LDA signal is given by:

$$\overline{\tilde{u}_{i0}(t)\tilde{u}_{j0}(t')} = \iiint\iiint_{all\ space} \overline{u_i(\vec{a},t)w(\vec{x}[\vec{a},t])u_j(\vec{a}',t')w(\vec{x}[\vec{a}',t'])}\ \overline{g(\vec{a})g(\vec{a}')}d^3\vec{a}\ d^3\vec{a}' \tag{7}$$

Since the initial positions of the particles (the $\vec{a}'s$) are truly independent of the field that transports them, the statistics of the g's and velocity field can be assumed to be statistically independent[1]. From before we already know that for the sampling function (cf., [3,5])

$$\overline{g(\vec{a})g(\vec{a}')} = \mu^2 + \mu\delta(\vec{a}' - \vec{a}) \tag{8}$$

This yields

$$\begin{aligned}\overline{\tilde{u}_{i0}(t)\tilde{u}_{j0}(t')} = \mu^2 \iiint\iiint_{all\ space} \overline{[u_i(\vec{a},t)w(\vec{x}[\vec{a},t])][u_j(\vec{a}',t')w(\vec{x}[\vec{a}',t'])]}d^3\vec{a}\ d^3\vec{a}' \\ + \mu\iiint_{all\ space} \overline{[u_i(\vec{a},t)w(\vec{x}[\vec{a},t])][u_j(\vec{a},t')w(\vec{x}[\vec{a},t'])]}d^3\vec{a}\end{aligned} \tag{9}$$

The double integral on the RHS is just the cross-correlation of the *instantaneous volume-averaged particle velocity at two times*; i.e.,

$$\mu^2 \iiint\iiint_{all\ space} \overline{[u_i(\vec{a},t)w(\vec{x}[\vec{a},t])][u_j(\vec{a}',t')w(\vec{x}[\vec{a}',t'])]}d^3\vec{a}\ d^3\vec{a}' = (\mu V)^2 \overline{\tilde{u}_{i0}^{vol}(t)\tilde{u}_{j0}^{vol}(t')} \tag{10}$$

As above, it corresponds to the two-time cross-correlation of the Eulerian velocities *only* if the scattering particles are following the flow.

The second integral is a consequence of the intermittency of the characteristic LDA off-on signal; see Velte et al. [10] or Chapter 10 in [4]. The quantity under the integral sign is evaluated for only a single particle, since it requires the initial particle position to be the same ($\vec{a}' = \vec{a}$) and the particle spends only a very short time in the scattering volume, t' $\approx$ t. So to the level of our measuring equipment, the entire expression can be approximated by:

$$\mu\iiint_{all\ space} \overline{[u_i(\vec{a},t)w(\vec{x}[\vec{a},t])][u_j(\vec{a},t')w(\vec{x}[\vec{a},t'])]}d^3\vec{a} \approx \mu V \left[\overline{\tilde{u}_{i0}^{vol}(t)\tilde{u}_{j0}^{vol}(t)}\right] \tag{11}$$

where we have assumed that $[w(\vec{x})]^2 \approx w(\vec{x})$, since it is usually just `1´ or `0´ (This is why the integral produces a V, not a V^2). Note that the quantity $\left[\overline{\tilde{u}_{i0}^{vol}(t)\tilde{u}_{j0}^{vol}(t)}\right]$ still includes both the mean and fluctuating components, so it can be very large indeed. The reason why this term becomes so large is just a consequence of subtracting off the wrong mean, since the mean value of the signal, $\bar{u}$, and the interrupted signal mean, $\bar{u}_0$, typically differ considerably, see Figure 1. Thus expression (9) simplifies to:

$$\overline{\tilde{u}_{i0}(t)\tilde{u}_{j0}(t')} \approx (\mu V)^2\ \overline{\tilde{u}_{i0}^{vol}(t)\tilde{u}_{j0}^{vol}(t')} + \mu V\ \left[\overline{\tilde{u}_{i0}^{vol}(t)\tilde{u}_{j0}^{vol}(t)}\right]\ \delta(t'-t) \tag{12}$$

---

[1] Note that this uncoupling is crucial, since otherwise the sampling process and sampled process are not statistically independent, which means the statistics are in principle biased. Note also that no arbitrary assumptions (e.g. Poisson-distributed, etc.) are necessary to derive the residence-time weighted algorithms, quite unlike competing bias correction schemes. In effect, by this approach the bias is simply avoided.

where the second term on the RHS contains the added variance and the random noise arising from the random arrivals which is uncorrelated with itself at all but zero time-lag where the correlation is perfect. As first noted by [7] (see also [3,5]), the second term produces a noise spike in the origin of the autocorrelation or, respectively, white noise in the spectrum. The effect of this term must be removed, for example, when computing the autocorrelation directly from the LDA data using the time-slot technique (see [3]). Thus the origin is avoided and the correlation there can only be obtained by extrapolating the rest of the curve to τ=0. This was the approach first employed using residence-time weighting by Buchhave [3].

4. Practical spectral estimator

This section will consider only the streamwise velocity spectra, although the methodology applies to all cross-spectra. The spectral estimator (originally derived by [3,6] and corrected by [4]) can be written in short form as:

$$S(f)=\frac{1}{(\mu V)^2}S^B_{0_T}(f) \;=\; \frac{T^2}{\left(\sum_{n=0}^{N-1}\Delta t_n\right)^2}\frac{\left|\hat{u}_{iT}(f)\right|^2}{T} \tag{13}$$

The factor $1/(\mu V)^2 = T^2/\left(\sum_{n=0}^{N-1}\Delta t_n\right)^2$ compensates for the fact that there is signal only when a particle is in the measuring volume (as shown in equation 12). Like all spectral estimators (and as shown later when the variability is considered), this one too must be either smoothed or block-averaged to produce converged statistics.

Substituting for the discretized Fourier transform using equation (6) yields:

$$S(f)=\frac{T}{\left(\sum_{n=0}^{N-1}\Delta t_n\right)^2}\sum_{\substack{m=0\\ m\neq n}}^{N-1}\sum_{n=0}^{N-1}e^{-i2\pi f(t_m-t_n)}u_m u_n \Delta t_m \Delta t_n \tag{14}$$

which is exactly the estimator originally employed by [3]. The problem, of course, is that the spectrum of the signal is completely swamped by the intermittency noise. Note that the frequencies can be chosen arbitrarily since the Fourier transform is computed using the Discrete-Time Fourier Transform (DTFT).

As noted above, the double summation algorithm of equation (14) was first employed by [3], who tried to remove the self-noise by eliminating the self-products (m=n terms). The results, however, were not very satisfactory. In part this was because the total length of the record was kept short in order to reduce the computational load of the double summation, and as a result the spectra were dominated by finite window effects. George [6] suggested that the computations could be significantly reduced by computing first the direct transform of equation (6), then squaring the result and subtracting off the contribution of the diagonal which was computed separately. This produced the same result with more efficiency and for longer records, but suffered from fact that both sums had to be computed to great accuracy, since the difference of two large numbers was desired. In fact both approach can be shown to be incorrect.

It was discovered in the course of this work that both approaches have the unintended result of completely removing the signal variance so that the resulting spectrum integrates to zero energy. Thus ***a major contribution of this work*** is the recognition that the spectrum computed from equation (14) (whether by doing the double sum without m=n terms, or using equation 6 first then subtracting the diagonal) must be corrected for this absence by offsetting all values by an additive constant so that its high frequency asymptote is zero [4,10].[2] This is exactly equivalent to adding back the turbulence energy, but without the self-realization noise. This procedure will be illustrated in the examples and figures below.

5. Experimental setups and results[3]

The algorithms above were applied to the burst mode data from two separate experiments: the far axisymmetric jet [9,11] and the two-dimensional cylinder wake of [12].

The Jet The experimental details for the axisymmetric turbulent far jet experiment can be found in [11]. This data includes simultaneously acquired hot-wire (HWA) and LDA data including the residence times from measurements performed in an axisymmetric turbulent far jet 30.3 diameters downstream of the jet exit. The sampling frequency for the HWA data was f_s = 40 000 Hz, which was well above the filter cutoff due to the length of the hot-wires (approximately 5 kHz). The average data rate for the LDA data was substantially lower at ν = 318 Hz.

Figures 2 (logarithmic plot) and 3 (linear plot) show the uncorrected and noise corrected burst-mode LDA spectra for the axisymmetric jet along with a spectrum from simultaneously acquired HWA data. The upper curve shows the burst-mode LDA spectrum if the diagonal terms are included in the computation; i.e. the self-noise is retained. The desired spectral content is essentially buried by the self-noise. By contrast, there is good agreement between the noise-corrected burst-mode LDA and HWA spectra up to a frequency of about 400 Hz, where the variability dominates the residual burst-mode LDA spectrum. The results could have been improved further by iterating on the amount by which the spectrum was shifted so as to bring the noise level to exactly zero. Clearly better statistical convergence (i.e., more measurement data) can assist in this iteration by providing a smoother spectral reference level.

The Wake In this experiment HWA data and LDA data including residence times were acquired under similar conditions in the wake of a circular cylinder in a wind tunnel at DTU[4]. The experimental setup for both is approximately the same as described by [12]. However, some important details are corrected and highlighted in the following. The circular cylinder had a diameter of 6 mm and was mounted in a square test section of width 300 mm in a closed loop wind tunnel. The material and mounting (firm or flexible) of the cylinder is unknown, however, it is known that it is some kind of metal and solid (as opposed to hollow). The HWA and LDA time series were acquired at the same position 26 mm downstream of the cylinder. The HWA measurements were acquired at a Reynolds number of 7 400 (U = 18.5 m/s) based on the cylinder diameter with a sampling frequency of f_s = 100 kHz. The Reynolds number for the LDA data is higher, 8 600 (U = 21.5 m/s) with an average data rate that is close to that of the HWA measurements, ν = 94 kHz. Thus the ratio of the mean velocities of the HWA and LDA data sets is U_{LDA}/U_{CTA} = 1.16, which is important to bear in mind when making comparisons. The spectra computed from these two data sets are compared despite the fact that they are acquired under slightly different conditions.

Figures 4 (logarithmic plot) and 5 (linear plot) show the wavenumber spectra (computed using Taylor's frozen field hypothesis) for the cylinder wake flow. Wavenumber spectra were used since the LDA and HWA measurements were, as mentioned above, acquired at slightly different Reynolds numbers. The reason why the spectral peaks do not line up is that the disturbance is

[2] As shown by Velte et al. [9], this exact procedure can in fact be used to produce noise-free spectra from virtually any signal, not just burst-mode LDA.

[3] All these datasets can be downloaded from http://ldvproc.nambis.de/

[4] These were kindly provided by Dr. Holger Nobach at Max-Planck Institut für Dynamik und Selbstorganisation. The HWA data set was downloaded from http://ldvproc.nambis.de/data/dtudata.html, while the LDA data were obtained directly from Holger Nobach.

temporal, not convected. This frequency corresponds to the eigenfrequency of the second vibrational mode of the solid cylinder [4]. The wavenumber spectra are shown to remove the effect of different free stream velocities if the spectra are normalized by the energy by similarity scaling for low wavenumbers (energy variables), i.e., by the factor $u^2L \sim U^2d$ [4]. Again, the noise corrected burst-mode LDA spectrum is shown to predict the spectrum well. Since the variability is less at the higher frequencies for this data (i.e., smaller values of the spectral estimator) due to the increased data rate and more blocks of data), it is possible to resolve more decades of the spectrum without iteration on the additive constant (see equation 15).

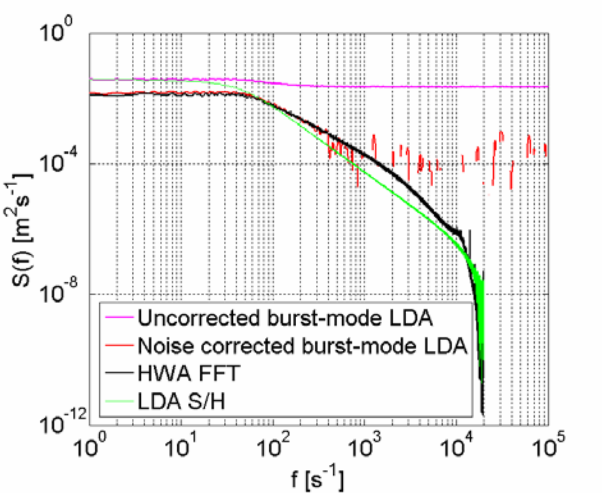

Figure 2: Comparison of burst-mode LDA, HWA and S/H spectra, axisymmetric jet.

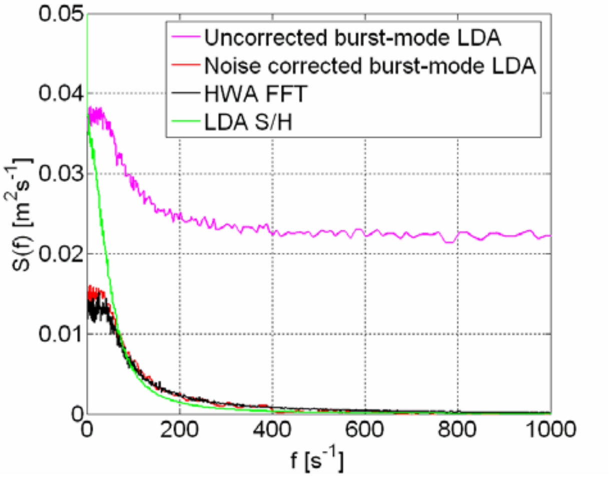

Figure 3: Comparison of burst-mode LDA, HWA and S/H spectra, axisymmetric jet.

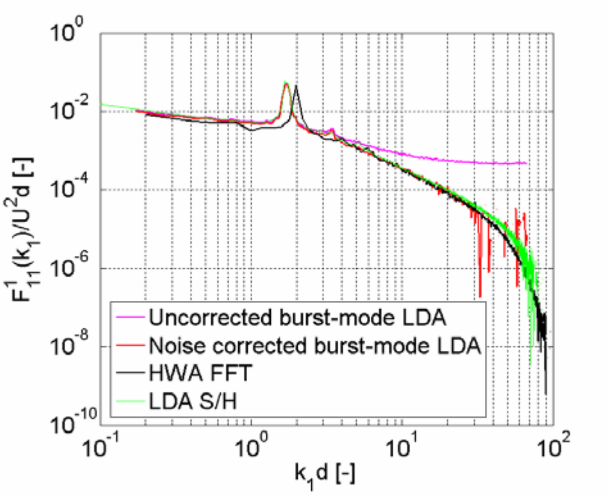

Figure 4: Comparison of burst-mode LDA, HWA and S/H spectra, cylinder wake.

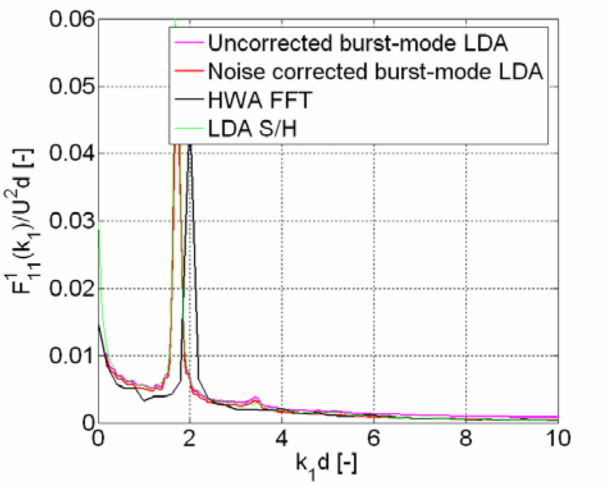

Figure 5: Comparison of burst-mode LDA, HWA and S/H spectra, cylinder wake.

6. Spectra computed by interpolating and re-sampling LDA data

Also shown for comparison in Figures 2-5 are spectra computed for the same data using standard FFT analysis on re-sampled data obtained from a continuous signal created by sample-and-hold from the same LDA burst-mode data. For the axisymmetric jet, the sample-and-hold spectrum is very different from both the hot-wire one and the one obtained from the LDA data using the residence-time burst-mode method described above. For the wake, there is very little difference except at high frequencies and at the very lowest frequencies. This is consistent with the analysis of Adrian and Yao [13], since the data density, $\nu\lambda_\tau$, is a measure of how many samples on average are taken during one Taylor microscale. This parameter is clearly critical for the performance of interpolation and re-sampling methods, as was pointed out in [3,4,13] and can also be seen in Figures 2-5. For the axisymmetric jet, $\nu\lambda_\tau$=0.7; therefore the re-sampled data cannot represent the signal very well [4]. Unless $\nu\lambda_\tau$ >>1, the spectra will be subject to frequency dependent noise, falling off as f^2 [3,13] for sample-and-hold (S/H), which is evident in Figure 2. Note that if not looking too carefully it would have been very easy to have confused the sample-and-hold spectrum with that of turbulence, when in fact is entirely determined by the spectra shape imposed upon it by the reconstruction. For the cylinder wake, the average sampling rate is substantially higher with a much higher data density $\nu\lambda_\tau$=94, so a better representation of the instantaneous signal is possible [4].

One can clearly see that, in contrast to the sample-and-hold spectra, the burst-mode LDA spectra collapse with the HWA spectra **independently** from data density. It is also worth stressing that the high data density required for the re-sampling methods to work is $\nu\lambda_\tau$ >> 1. This is typically a very difficult condition which can rarely be satisfied for LDA measurements, and failure to recognize the problem can seriously compromise the quality of the acquired data. Moreover, attempts to satisfy it experimentally risks violating the requirement of at most one particle at a time in the scattering volume. This would make it behave like a tracker, producing ambiguity noise [5]. Clearly only the burst-mode algorithm can reasonably be used for lower data rates.

7. Statistical convergence and sample size

The random sampling inherent in the burst-mode LDA measurement technique significantly affects the amount of data required to obtain converged burst-mode LDA spectra. If one relies on the assumption that the fourth order moments are jointly Gaussian, i.e., $\overline{uu'u''u'''} = \overline{uu'}\,\overline{u''u'''} + \overline{uu''}\,\overline{u'u'''} + \overline{uu'''}\,\overline{u'u''}$, then the variability of the spectral estimator for a single block of data can be shown to be given by (see Appendix A);

$$\varepsilon_S^2 = \frac{\mathrm{var}\{S(f)\}}{[S(f)]^2} = 1 + \frac{4}{\nu}\frac{B(0)}{S(f)} \tag{15}$$

where B(0) is the velocity variance (including self-noise [4,10]). When many blocks of data are averaged together, this variablity decreases by the inverse square root of number of independent data records used to produce the block-averaged spectrum. Clearly when S(f) drops (as it usually does at higher frequencies), the variability increases. Or said another way, the number of blocks of data required to achieve a given variability of the spectral estimator increases with decreased magnitude of the spectrum [1,14]. This is quite different that the usual spectra (i.e., not randomly sampled) for which the variability is frequency independent.

8. Practical considerations

Obviously it is crucial that whatever method is used to process the LDA signal burst, it must produce correct values of all three necessary parameters: u_{in}, Δt_n, and t_n. While both leading commercial processors produce reliable values of at least the velocity, there have been a variety of problems reported for Δt_n and t_n (e.g., [15,16]). The former [15] used older Dantec (DISA) counters, most versions of which (if unmodified) produced random numbers for the residence times due to overflow of the register used to count the pulses in a burst. To the best of our ability to determine the current Dantec burst processors used herein function correctly. Shiri [17] using the same hardware, however, encountered problems with the particle arrival times, t_n, when using very large data sets (>10,000 realizations) with multiple channels – the data reported from one channel appeared to skip several realizations, confusing the arrival times and which pairs of data belonged together. These were apparently due to buffer overflow, and easy to spot by comparing the arrival and residence times for both channels (which should be nearly the same). The cause of the problems encountered by [16] using TSI correlation processors were never really sorted out (to the best of our knowledge), but appeared to be due to an incorrect reading of the residence time data registers, and therefore an incorrect reassembling of the binary data. George [6] (see also [4,18]) discuss a number of useful diagnostics to make sure all these parameters have been correctly reported by the hardware. One of the most useful of these is to simply examine scatter plots of u_{in} versus Δt_n, which should have a characteristic banana shape. Large numbers of realizations with very small residences times suggest signal quality/processing is deficient. An alternative strategy (in fact ultimately used by [16] to overcome problems with their TSI processors) is to produce residence time data by simply recycling the burst processor for a fixed number of fringe-crossings (say 8 or 16) within the same burst as many times as possible, outputting each sub-burst immediately while recycling the processor to measure for another 8 or 16 fringe-crossings. The key is to use enough frequency shift to ensure that both the long and short residence times are well-represented in the data set. For such measurements, simple arithmetic averaging is equivalent to the residence-time weighted results, since the weighting is accounted for by the number of times a given burst is counted. Fourier analysis can be performed in the same manner, or by regrouping the data to reconstruct the actual burst. The latter reduces considerably the amount of data to be processed. Although functional, this approach is at best a crude fix to a hardware problem that should be correctable (at least by the manufacturer).

Due to the inherent random sampling, Fast Fourier Transform algorithms cannot be used to compute the direct Fourier transform of the burst mode velocity signal. Hence, the spectrum has to be computed by the direct Fourier transform (DTFT). This can be done by squaring the result of a single summation for selected frequencies, or by addressing the double summation directly. The latter is the most accurate (since it by eliminating the self-products in the computation, the self-noise never enters at all), but this approach requires a double sum to be performed over the entire block of data for each frequency. Matlab performs poorly in this situation, since it needs to re-allocate memory for every loop iteration. FORTRAN does not have this problem, since memory allocation for each element is done before entering the loops. But even when parallelizing the code, the double summation computational time can be hours or days for the data sets presented here, depending on record lengths and number of blocks used.

An alternative approach is to utilize the compiled matrix multiplication utility in Matlab. One can avoid loops by computing vectorized sums so that the element wise operations are made in one stroke using compiled functions. In addition, by pre-dimensioning the matrices, one can reduce the computational time even further. Using this method, the spectra presented here can be computed in a matter of say 10-15 minutes on a 1.2 GHz dual processor laptop. Note that the blocks should have the same record length, T, in physical units, so the number of samples per block might vary. Keeping T constant insures that the window function convolving the spectrum is constant. Further, it is also important to remember to subtract the (residence time weighted) mean velocity of each particular block, not that of the full time series. Obviously care should be taken to insure that blocks with wildly different values of the number of realization are eliminated from the analysis. A suggested sample Matlab code can be found in Appendix B.

Acknowlegements

The authors are especially grateful to Dr. Bettina Frohnapfel of the Technical U. of Darmstadt for providing the jet HWA and LDA data, and to Dr. Holger Nobach, Max-Planck Institut für Dynamik und Selbstorganisation, and Knud Erik Meyer, Technical University of Denmark, for providing the wake data. The authors also gratefully acknowledge many helpful discussions with T. Gunnar Johansson of Chalmers Technical University. This work formed a portion of the Ph.D. dissertation of CMV, who was supported by the Danish Research Council, DSF, under grant number 2104-04-0020. WKG acknowledges the support of Vetenskapsrådet (The Swedish Research Council). This work was carried out in part while WKG was an Otto Mønsted Visiting Professor at the Danish Technical University in 2007.

Appendix A: Derivation of variability

Below is given a summary of the derivation of the variability of the spectral estimator for randomly sampled data. A more detailed summary can be found in [4]. The fourth order moment of the random sampling function

$$\begin{aligned}\overline{gg'g''g'''} = \ & 1+\frac{1}{\nu}\left[\delta(t'-t)+\delta(t''-t)+\delta(t'''-t)+\delta(t''-t')+\delta(t'''-t')+\delta(t'''-t'')\right]+ \\ & \frac{1}{\nu^2}\left[\delta(t'-t)\delta(t''-t)+\delta(t'-t)\delta(t'''-t)+\delta(t'''-t)\delta(t''-t)+\delta(t'''-t')\delta(t''-t')\right]+ \\ & \frac{1}{\nu^3}\delta(t'-t)\delta(t''-t)\delta(t'''-t)\end{aligned} \tag{16}$$

is incorporated into the variance of the spectral estimator. This quantity can be derived by assuming that g, g′, g′′, g′′′ are uncorrelated, for which the following must hold true:

$$\begin{cases}\overline{(g-\nu)(g'-\nu)(g''-\nu)(g'''-\nu)} = \frac{1}{\nu^3}\delta(t'-t)\delta(t''-t)\delta(t'''-t) \\ \overline{(g-\nu)(g'-\nu)(g''-\nu)} = \frac{1}{\nu^2}\delta(t'-t)\delta(t''-t) \\ \overline{(g-\nu)(g'-\nu)(g'''-\nu)} = \frac{1}{\nu^2}\delta(t'-t)\delta(t'''-t) \\ \overline{(g-\nu)(g''-\nu)(g'''-\nu)} = \frac{1}{\nu^2}\delta(t''-t)\delta(t'''-t) \\ \overline{(g'-\nu)(g''-\nu)(g'''-\nu)} = \frac{1}{\nu^2}\delta(t''-t')\delta(t'''-t')\end{cases} \tag{17}$$

$$\begin{cases}\overline{(g-\nu)(g'-\nu)} = \frac{1}{\nu}\delta(t'-t) \\ \overline{(g-\nu)(g''-\nu)} = \frac{1}{\nu}\delta(t''-t) \\ \overline{(g-\nu)(g'''-\nu)} = \frac{1}{\nu}\delta(t'''-t) \\ \overline{(g'-\nu)(g''-\nu)} = \frac{1}{\nu}\delta(t''-t') \\ \overline{(g'-\nu)(g'''-\nu)} = \frac{1}{\nu}\delta(t'''-t') \\ \overline{(g''-\nu)(g'''-\nu)} = \frac{1}{\nu}\delta(t'''-t'')\end{cases} \tag{18}$$

Expanding the first equation in (17), one can solve for $\overline{gg'g''g'''}$. Similarly expanding the remaining in (17) and (18) and substituting these into the first, one obtains (16).

Assuming that the sampling process is independent of the process being sampled and that the fourth order moments of the velocities are jointly Gaussian;

$$\mathrm{var}\left\{S_T^R(f)\right\} = \left\langle \frac{1}{T^2} \int_{-T/2}^{T/2} \int_{-T/2}^{T/2} \int_{-T/2}^{T/2} \int_{-T/2}^{T/2} e^{-i2\pi f\left[(t-t')+(t''-t''')\right]} uu'u''u''' gg'g''g'''\, dt\, dt'\, dt''\, dt''' \right\rangle =$$
$$\frac{1}{T^2} \int_{-T/2}^{T/2} \int_{-T/2}^{T/2} \int_{-T/2}^{T/2} \int_{-T/2}^{T/2} e^{-i2\pi f\left[(t-t')+(t''-t''')\right]} \left[\overline{uu'}\,\overline{u''u'''} + \overline{uu''}\,\overline{u'u'''} + \overline{uu'''}\,\overline{u'u''}\right] \overline{gg'g''g'''}\, dt\, dt'\, dt''\, dt''' \tag{19}$$

where the superscript indicates that the estimator is valid for random sampling. Now by inserting the fourth order moment of the sampling function (16) and using the following fundamental properties of the generalized Dirac delta function;

$$\int_{-\infty}^{\infty} \delta(t-t_0)\,dt \equiv 1 \tag{20}$$

$$\delta(t) = 0, \quad t \neq 0 \tag{21}$$

$$\int_{-\infty}^{\infty} f(t)\delta(t-t_0)\,dt = f(t_0) \tag{22}$$

and solving the integrals in the limit as the record length goes to infinity, one obtains the final result:

$$\varepsilon_S^2 = \frac{\mathrm{var}\{S(f)\}}{[S(f)]^2} = 1 + \frac{4}{\nu}\frac{B(0)}{S(f)} \tag{23}$$

Appendix B: Proposed Matlab-algorithm

```
load u; load t; load tt;   %% Load velocities, arrival times and transit times

bl = 1500;                 %% Number of blocks
M = 600;                   %% Number of frequencies
f = logspace(0,5,M);       %% Define frequencies
T_b = 1.0;                 %% Block record length [s]

blocklength = linspace(1,bl+1,bl+1)*T_b; %% Set block record length
ii(1) = 1;      %% Index of first element in block
for k=1:bl+1
     %% Determine ii - start index for each block
     [rte(k),ii(k+1,1)] = min(abs(t - blocklength(k)));
     %% RTW average of u for each block
     umean(k) = sum(u(ii(k):ii(k+1)-1).*tt(ii(k):ii(k+1)-1))/ (sum(tt(ii(k):ii(k+1)-1)));
     %% Obtain velocity fluctuations
     u(ii(k):ii(k+1)-1) = u(ii(k):ii(k+1)-1)-umean(k);
end
utt = u.*tt;              %% Element-wise multiplication of the velocities and transit times
N = max(diff(ii))+1; %% Maximum number of samples in a block

%% Pre-dimension matrices to reduce memory handling resources
E = zeros(M,1);
S_bl = zeros(M,bl);
f_tot = repmat(f',1,N);

%% Compute one spectrum for each block
for k=1:bl
    WN = exp(-i*2*pi*repmat(t(ii(k):ii(k+1)-1),length(f),1).*f_tot(:,1:ii(k+1)-ii(k))) * utt(ii(k):ii(k+1)-1)';
    S_bl(:,k)=(t(ii(k+1)-1)-t(ii(k)))*abs(WN.*conj(WN))/(sum(tt(ii(k):ii(k+1)-1))^2);
end
S=mean(S_bl,2);   %% Average the spectra for all blocks
```

9. References

[1] George WK; Beuther PD; Lumley JL (1978) Processing of Random Signals. Proceedings of the Dynamic Flow Conference, Skovlunde, Denmark, (PO Box 121, DK-2740 Skovlunde), 757–800.

[2] Albrecht HE; Borys M; Damaschke N; Tropea C (2003) Laser Doppler and Phase Doppler Measurement Techniques. Springer-Verlag, Berlin, Heidelberg.

[3] Buchhave P (1979) Errors and Correction Methods in Turbulence Measurements with the LDA. Ph.D. Dissertation. State University of New York at Buffalo.

[4] Velte CM (2009) Characterization of Vortex Generator Induced Flow. Ph.D. Dissertation. Technical University of Denmark.

[5] Buchhave P; George WK; Lumley JL (1979) The Measurement of Turbulence with the Laser-Doppler Anemometer. Ann. Rev. Fluid Mech. 11, 443-504.

[6] George WK (1988) Quantitative Measurement with the Burst-Mode Laser Doppler Anemometer. Exp. Ther. Fluid Sc. 1, 29-40.

[7] George WK (1976) Limitations to Measuring Accuracy Inherent in the Laser Doppler Signal. The Accuracy of Flow Measurements by Laser Doppler Methods, Proceedings LDA Symposium, Copenhagen, 1975 (Buchhave et al. eds.), pp. 20-63, Dantec, DK-2740, Skovlunde, Denmark.

[8] Collins LR; Keswani A (2004) Reynolds Number Scaling of Particle Clustering in Turbulent Aerosols. New J. Phys. 6, 119.

[9] Ewing D; Frohnapfel B; George WK; Pedersen JM; Westerweel J (2007) Two-Point Similarity in the Round Jet, J. Fluid Mech. 577, 309-330.

[10] Velte CM; Tutkun M; George WK (2010) New Correction for Random Noise in Spectra, submitted for publication.

[11] Frohnapfel B (2003) Multi-point similarity of the axisymmetric turbulent far jet and its implications for the POD. M.Sc. thesis. Chalmers University of Technology and Friedrich-Alexander- Universität.

[12] Gjelstrup P; Nobach H; Jørgensen FE; Meyer KE (2000) Experimental verification of novel spectral analysis algorithms for Laser Doppler Anemometry data. Proc. 10th Int. Symp. Appl. Laser Tech. Fluid Mech., July 10–13, Lisbon, Portugal.

[13] Adrian RJ; Yao CS (1987) Power spectra of fluid velocities measured by laser doppler velocimetry. Exp. Fluids 5, 17–28.

[14] Gaster M; Roberts JB (1975) Spectral analysis of randomly sampled signals. J. Inst. Math. App. 15, 195–216.

[15] Hussein HJ; Capp SP; George WK (1994) Velocity measurements in a high-Reynolds-number, momentum-conserving, axisymmetric, turbulent jet, J. Fluid Mech. 258, 31-75.

[16] Eriksson JG; Karlsson RI; Persson J (1998) An experimental study of a two-dimensional plane turbulent wall jet, Exp. Fluids 25, 50-60.

[17] Shiri, A. (2010) Chalmers U. of Tech., private communication to WKG.

[18] Capp SP (1983) Experimental investigation of the turbulent axisymmetric jet. Ph.D. Dissertation. State University of New York at Buffalo.